Journal of Sound and Vibration (1998) **216**(2), 251–267
Article No. sv981667

ISOLATION DESIGN FOR A FLEXIBLE SYSTEM

D. SCIULLI

Air Force Research Laboratory, *AFRL/VSDV*, 3550 *Aberdeen Ave*. *SE*, *Kirtland AFB*, *NM* 87117, *U.S.A*.

AND

D. J. INMAN

Engineering Science and Mechanics, *Virginia Polytechnic Institute & State University*, *Blacksburg*, *VA* 24061-0219, *U.S.A*.

(*Received* 11 *August* 1997, *and in final form* 15 *March* 1998)

It has been commonly assumed that the corner or mount frequency in an isolator should be designed as low as possible. This is one result of using a single-degree-of-freedom (SDOF) system to model isolation systems. However, for systems that have flexible or non-rigid foundations, a design point for the mount frequency can occur between the modes of the base. By implementing this type of design, a strong interaction will exist between the modes. When isolator damping is included, whether done passively or actively, more than one mode can be attenuated by this new mount design. Therefore, the effects of the mount frequency on isolation designs are discussed as well as using both passive and active damping in the isolator. For active damping, three commonly used control methodologies are discussed: a proportional-plus-integral-plus-derivative ($\mathscr{PID}$) controller, a linear quadratic Gaussian (LQG) regulator and a positive position feedback (PPF) controller.

1. INTRODUCTION

There have been numerous publications that have used a single-degree-of-freedom (SDOF) system to model both active and passive isolators [1–4]. The SDOF model consists of a rigid equipment mounted by some sort of isolator to a rigid, massless base. These assumptions are used to obtain a very simple calculation for the transmissibility. However, there are cases when the base is not rigid but flexible and its influence on the transmissibility must be determined. Several authors [5, 6] have looked at base flexibility; however, they used approximate techniques to solve the isolation problem. Blackwood looked at base flexibility as a perturbation to a rigid base solution, while Snowdon analyzed a symmetrical isolation system. Also, these authors did not fully explore the effect of the mount frequency on the isolation design.

This paper will use a method developed by Yang [7] to solve complex distributed parameter systems, such as the flexible base, rigid equipment (FBRE) isolation problem. This method will result in an exact solution to the FBRE system; therefore, it avoids standard truncation errors that are found in current literature. The flexibility in the base will be modeled as a Bernoulli–Euler beam and the beam damping will be modelled as proportional damping. It will be shown that the design point for the mount frequency in the FBRE system does not necessarily have to be as low as possible for best results. If the mount frequency lies between the base modes, a strong interaction between the modes

0022–460X/98/370251 + 17 $30.00/0

will exist. When isolator damping is included in the isolator, whether done actively or passively, multiple modes can be attenuated.

2. SINGLE-DEGREE-OF-FREEDOM MODEL

A brief discussion of the SDOF model for vibration isolation will be described since subsequent sections will compare results of the FBRE system with the SDOF model. It is well known and understood that attenuation of the transmissibility will occur at the point $\sqrt{2}\omega_o$, where ω_o is the corner or mount frequency of the isolator; amplification will occur in the region below this point. The transmissibility (T) is defined as the complex ratio of the equipment vibratory displacement to the vibratory displacement of the beam at the isolator attachment point. When viscous damping is included in the isolator, the transmissibility is reduced at the resonant condition from a theoretical infinite value to a finite value. However, the transmissibility for frequencies greater than $\sqrt{2}\omega_o$ will be increased compared to an undamped system. There is still attenuation in this frequency range but at a smaller level. Figure 1 shows the transmissibility for an undamped isolator and an isolator having a 20% damping ratio (ζ) using passive and active isolators. The high isolator damping in the passive system is used to show the increase of transmissibility at high frequencies compared to a system with no damping.

Since passive isolators tend to increase the high frequency transmissibility, active isolators are a good alternative. An active isolator can be designed to add damping at the resonant condition without increasing the high frequency transmissibility. As seen from Figure 1, active isolation has the same level of damping at the resonant condition compared to a damped passive isolator. Also, the high frequency transmissibility for the active isolator tracks the transmissibility of an undamped passive isolator.

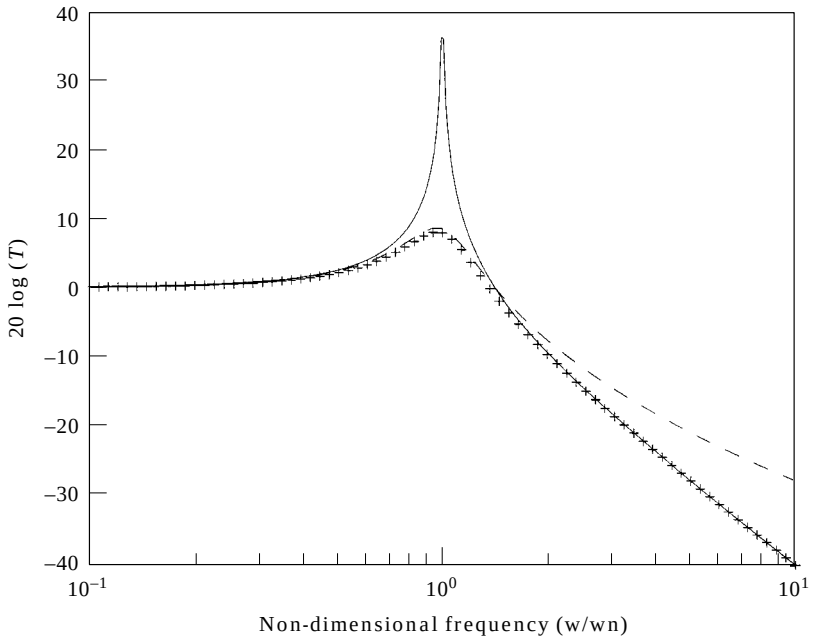

Figure 1. Absolute transmissibility plots for SDOF model (−, passive $\zeta = 0$: +, active $\zeta = 0{\cdot}2$; —, passive $\zeta = 0{\cdot}2$).

3. YANG'S METHOD

As mentioned previously, Yang developed a method to analyze complex one-dimensional systems exactly. Unlike approximate methods, such as the assumed modes method [8] or impedance methods [6, 9], no knowledge of the eigenvalues or mode shapes are needed to model flexible systems. In fact, Yang's method is somewhat similar to the finite element method because it can be used to find the eigensolutions for a particular system. His method is briefly described in the following sections.

3.1. SINGLE-SYSTEM RESPONSE

An nth-order, linear distributed parameter system response, $W(x, t)$, can be described by the following equation which is nondimensional in the spatial variable:

$$\left\{A\frac{\partial^2}{\partial t^2} + B\frac{\partial}{\partial t} + C\right\}W(x, t) = f(x, t), \qquad x\in(0, 1), \quad t > 0, \tag{1}$$

where A, B, and C are spatial differential operators that are equivalent to

$$A = \sum_{k=0}^{n} a_k \frac{\partial^k}{\partial x^k}, \qquad B = \sum_{k=0}^{n} b_k \frac{\partial^k}{\partial x^k}, \qquad C = \sum_{k=0}^{n} c_k \frac{\partial^k}{\partial x^k}. \tag{2}$$

The constants a_k, b_k, and c_k can represent inertia, damping, distributed constraints, Coriolis acceleration, axial loads, mass transport, centrifugal forces and circulatory effects; the term $f(x, t)$ is the external disturbance.

The system has inhomogeneous boundary conditions represented by

$$M_j W(x, t)|_{x=0} + N_j W(x, t)|_{x=1} = \gamma_j(t), \qquad t \geqslant 0, \quad j = 1, 2, \ldots, n, \tag{3}$$

where M_j and N_j are linear, temporal, spatial, differential operators. $\gamma_j(t)$ are known functions representing the external disturbances at the boundaries.

The Laplace transform of equation (1) with respect to time is

$$\{s^2A + sB + C\}\,\bar{W}(x, s) = \bar{f}(x, s), \tag{4}$$

where $\bar{(\,)}$ represents a Laplace transformation and the initial conditions were neglected. The boundary conditions in the Laplace domain are

$$\bar{M}_j\bar{W}(x, s)|_{x=0} + \bar{N}_j\bar{W}(x, s)|_{x=1} = \bar{\gamma}(s) = \bar{\gamma}_j(s) + \bar{\gamma}_{Ij}(s), \qquad j = 1, 2, \ldots, n. \tag{5}$$

$\bar{\gamma}_{Ij}$ is a polynomial in s representing the initial conditions at the boundaries.
Equation (4) can be recast into state space form as

$$\frac{\partial}{\partial x}\boldsymbol{\eta}(x, s) = \underline{\mathbf{F}}(s)\boldsymbol{\eta}(x, s) + \mathbf{f}(x, s), \qquad \underline{\mathbf{M}}(s)\boldsymbol{\eta}(0, s) + \underline{\mathbf{N}}(s)\boldsymbol{\eta}(1, s) = \boldsymbol{\gamma}(s). \tag{6a, b}$$

where

$$\boldsymbol{\eta}(x, s) = \begin{Bmatrix} \bar{W}(x, s) \\ \dfrac{\partial\bar{W}(x, s)}{\partial x} \\ \vdots \\ \dfrac{\partial^{n-1}\bar{W}(x, s)}{\partial x^{n-1}} \end{Bmatrix}, \qquad \mathbf{f}(x, s) = \begin{Bmatrix} 0 \\ 0 \\ \vdots \\ \dfrac{\bar{f}(x, s)}{a_n s^2 + b_n s + c_n} \end{Bmatrix}, \qquad \boldsymbol{\gamma}(s) = \begin{Bmatrix} \bar{\gamma}_1(s) \\ \bar{\gamma}_2(s) \\ \vdots \\ \bar{\gamma}_n(s) \end{Bmatrix}.$$

$\underline{\mathbf{F}}(s)$ is defined as

$$\underline{\mathbf{F}}(s) = \begin{bmatrix} 0 & 1 & 0 & \cdots & 0 \\ 0 & 0 & 1 & 0 & 0 \\ \vdots & \ddots & \ddots & \ddots & 0 \\ 0 & \cdots & \cdots & 0 & 1 \\ d_o(s) & d_1(s) & \cdots & \cdots & d_k(s) \end{bmatrix}, \tag{7}$$

and the coefficients of the matrix $\underline{\mathbf{F}}(s)$ are

$$d_k(s) = -\frac{a_k s^2 + b_k s + c_k}{a_n s^2 + b_n s + c_n}, \qquad k = 0, 1, \ldots, n-1. \tag{8}$$

The solution to equation (6a), given the boundary conditions in equation (6b) are

$$\boldsymbol{\eta}(x, s) = \int_0^1 \underline{\mathbf{G}}(x, \xi, s)\mathbf{f}(\xi, s)\, \mathrm{d}\xi + \underline{\mathbf{H}}(x, s)\boldsymbol{\gamma}(s), \qquad x \in (0, 1), \tag{9}$$

where

$$\underline{\mathbf{G}}(x, \xi, s) = \begin{cases} \mathrm{e}^{\underline{\mathbf{F}}(s)x}[\underline{\mathbf{M}}(s) + \underline{\mathbf{N}}(s)\,\mathrm{e}^{\underline{\mathbf{F}}(s)}]^{-1}\underline{\mathbf{M}}(s)\,\mathrm{e}^{-\underline{\mathbf{F}}(s)\xi}, & \xi < x, \\ -\mathrm{e}^{\underline{\mathbf{F}}(s)x}[\underline{\mathbf{M}}(s) + \underline{\mathbf{N}}(s)\,\mathrm{e}^{\underline{\mathbf{F}}(s)}]^{-1}\underline{\mathbf{N}}(s)\,\mathrm{e}^{\underline{\mathbf{F}}(s)(1-\xi)}, & \xi > x, \end{cases} \tag{10a}$$

$$\underline{\mathbf{H}}(x, s) = \mathrm{e}^{\underline{\mathbf{F}}(s)x}[\underline{\mathbf{M}}(s) + \underline{\mathbf{N}}(s)\,\mathrm{e}^{\underline{\mathbf{F}}(s)}]^{-1}. \tag{10b}$$

3.2. SUBSYSTEM RESPONSE

The solution in equation (9) is valid for a single system; therefore, this section will describe the solution for an arbitrary number of interconnected systems, i.e., subsystems. For each subsystem, the displacement and strain vectors can be defined as

$$\boldsymbol{\alpha}(x, s) = \begin{Bmatrix} W(x, s) \\ \dfrac{\partial W(x, s)}{\partial x} \\ \vdots \\ \dfrac{\partial^{(n/2)-1} W(x, s)}{\partial x^{(n/2)-1}} \end{Bmatrix}, \qquad \boldsymbol{\varepsilon}(x, s) = \begin{Bmatrix} \dfrac{\partial^{n/2} W(x, s)}{\partial x^{n/2}} \\ \dfrac{\partial^{(n/2)+1} W(x, s)}{\partial x^{(n/2)+1}} \\ \vdots \\ \dfrac{\partial^{n-1} W(x, s)}{\partial x^{n-1}} \end{Bmatrix}, \tag{11}$$

where $\boldsymbol{\eta} = \{\boldsymbol{\alpha}^T(x, s)\ \boldsymbol{\varepsilon}^T(x, s)\}^T$. The internal force vector of each subsystem, $\mathbf{P}(x, s)$, is described by

$$\mathbf{P}(x, s) = \underline{\mathbf{E}}(s)\boldsymbol{\varepsilon}(x, s), \tag{12}$$

where $\underline{\mathbf{E}}(s)$ is a constitutive matrix. If $\boldsymbol{\gamma}(s)$, $\underline{\mathbf{M}}(s)$, and $\underline{\mathbf{N}}(s)$ are defined as

$$\boldsymbol{\gamma}(s) = \begin{Bmatrix} \boldsymbol{\alpha}_0(s) = \boldsymbol{\alpha}(0, s) \\ \boldsymbol{\alpha}_1(s) = \boldsymbol{\alpha}(1, s) \end{Bmatrix}, \qquad \underline{\mathbf{M}}(s) = \begin{bmatrix} \underline{\mathbf{I}} & \underline{\mathbf{0}} \\ \underline{\mathbf{0}} & \underline{\mathbf{0}} \end{bmatrix}, \qquad \underline{\mathbf{N}}(s) = \begin{bmatrix} \underline{\mathbf{0}} & \underline{\mathbf{0}} \\ \underline{\mathbf{I}} & \underline{\mathbf{0}} \end{bmatrix},$$

the solution of each subsystem in local coordinates becomes

$$\boldsymbol{\alpha}(x, s) = \int_0^1 \underline{\mathbf{G}}_\alpha(x, \xi, s)\mathbf{f}(\xi, s)\,\mathrm{d}\xi + \underline{\mathbf{H}}_{\alpha 0}(x, s)\boldsymbol{\alpha}_0(s) + \underline{\mathbf{H}}_{\alpha 1}(x, s)\boldsymbol{\alpha}_1(s), \tag{13a}$$

$$\mathbf{P}(x, s) = \underline{\mathbf{E}}(s)\left\{\int_0^1 \underline{\mathbf{G}}_\varepsilon(x, \xi, s)\mathbf{f}(\xi, s)\,\mathrm{d}\xi + \underline{\mathbf{H}}_{\varepsilon 0}(x, s)\boldsymbol{\alpha}_0(s) + \underline{\mathbf{H}}_{\varepsilon 1}(x, s)\boldsymbol{\alpha}_1(s)\right\}. \tag{13b}$$

$\underline{\mathbf{G}}_\alpha$, $\underline{\mathbf{G}}_\varepsilon$, $\underline{\mathbf{H}}_{\alpha 0}$, $\underline{\mathbf{H}}_{\alpha 1}$, $\underline{\mathbf{H}}_{\varepsilon 0}$ and $\underline{\mathbf{H}}_{\varepsilon 1}$ are partitioned matrices of equation (10).

3.3. SUBSYSTEM ASSEMBLY

Suppose there are N nodes where Z subsystems are interconnected and define the global displacements at each node by $\mathbf{u}_k$. The global nodal force of each subsystem is designated by $\mathbf{Q}_k^\delta$, where k is a particular node and δ is a given subsystem. At each mode there can be constraint forces and external disturbances designated by $\underline{\mathbf{C}}_k$ and $\mathbf{p}_k$, respectively. The constraint matrix, $\underline{\mathbf{C}}_k$, is valid only for connection of lumped systems or distributed systems at a single point. The force balance of the Z subsystems at node l is

$$\mathbf{Q}_l^A(s) + \mathbf{Q}_l^B(s) + \mathbf{Q}_l^C(s) + \cdots + \mathbf{Q}_l^Z(s) - \underline{\mathbf{C}}_l(s)\mathbf{u}_l(s) + \mathbf{p}_l(s) = \mathbf{0}. \tag{14}$$

The global force vector of subsystem δ at node l is defined as

$$\mathbf{Q}_l^\delta(s) = -\underline{\mathbf{R}}^\delta\mathbf{P}^\delta(x_l, s), \tag{15}$$

where $\underline{\mathbf{R}}^\delta$ is the transformation matrix of the local forces to global forces. However, the local forces, $\mathbf{P}^\delta(x_l, s)$, are defined in local coordinates and these coordinates need to be transformed as well. The transformation of the local displacements to global coordinates is accomplished with the transformation matrices $\underline{\mathbf{S}}^\delta$ and $\underline{\mathbf{T}}^\delta$ which are defined at either end of subsystem δ:

$$\boldsymbol{\alpha}^\delta(x_l, s) = \underline{\mathbf{S}}^\delta\mathbf{u}_l(s), \qquad \boldsymbol{\alpha}^\delta(x_i, s) = \underline{\mathbf{T}}^\delta\mathbf{u}_i(s). \tag{16}$$

Placing equation (13b) and equation (16) into equation (15) gives the global force vector in terms of global coordinates:

$$\mathbf{Q}_l^\delta(s) = -\underline{\mathbf{K}}_{ll}^\delta(s)\mathbf{u}_l(s) - \underline{\mathbf{K}}_{li}^\delta\mathbf{u}_i(s) - \mathbf{f}_l^\delta(s). \tag{17}$$

This equation assumes that $x_i < x_l$; otherwise, the equations below need to be redefined. The matrices in equation (17) are

$$\underline{\mathbf{K}}_{li}^\delta(s) = \underline{\mathbf{R}}^\delta\underline{\mathbf{H}}_{\varepsilon 0}(x_l, s)\underline{\mathbf{T}}^\delta, \qquad \underline{\mathbf{K}}_{ll}^\delta(s) = \underline{\mathbf{R}}^\delta\underline{\mathbf{H}}_{\varepsilon 1}(x_l, s)\underline{\mathbf{S}}^\delta,$$

$$\mathbf{f}_l^\delta(s) = \underline{\mathbf{R}}^\delta\underline{\mathbf{E}}^\delta(s)\int_0^1 \underline{\mathbf{G}}_\varepsilon^\delta(x_l, \xi, s)\mathbf{f}^\delta(\xi, s)\,\mathrm{d}\xi. \tag{18}$$

With this result, the global forces of each subsystem connected at node l are

$$\begin{aligned}
\mathbf{Q}_l^A(s) &= -\underline{\mathbf{K}}_{ll}^A(s)\mathbf{u}_l(s) - \underline{\mathbf{K}}_{li}^A(s)\mathbf{u}_i(s) - \mathbf{f}_l^A(s),\\
\mathbf{Q}_l^B(s) &= -\underline{\mathbf{K}}_{ll}^B(s)\mathbf{u}_l(s) - \underline{\mathbf{K}}_{lj}^B(s)\mathbf{u}_j(s) - \mathbf{f}_l^B(s),\\
&\vdots\\
\mathbf{Q}_l^Z(s) &= -\underline{\mathbf{K}}_{ll}^Z(s)\mathbf{u}_l(s) - \underline{\mathbf{K}}_{lm}^Z(s)\mathbf{u}_m(s) - \mathbf{f}_l^Z(s).
\end{aligned} \tag{19}$$

Note that these equations automatically satisfy displacement compatibilities at node l. Placing equation (19) into equation (14) yields

$$\underline{\mathbf{K}}_{ll}(s)\mathbf{u}_l(s) + \underline{\mathbf{K}}_{li}(s)\mathbf{u}_i(s) + \underline{\mathbf{K}}_{lj}(s)\mathbf{u}_j(s) + \cdots + \underline{\mathbf{K}}_{lm}(s)\mathbf{u}_m(s) = \mathbf{q}_l(s), \tag{20}$$

where

$$\begin{gathered}\underline{\mathbf{K}}_{ll}(s) = \underline{\mathbf{C}}_l(s) + \underline{\mathbf{K}}_{ll}^A(s) + \underline{\mathbf{K}}_{ll}^B(s) + \cdots + \underline{\mathbf{K}}_{ll}^Z(s),\\ \underline{\mathbf{K}}_{li}(s) = \underline{\mathbf{K}}_{li}^A(s), \qquad \underline{\mathbf{K}}_{lj}(s) = \underline{\mathbf{K}}_{lj}^B(s)\,, \ldots, \underline{\mathbf{K}}_{lm}(s) = \underline{\mathbf{K}}_{lm}^Z(s),\\ \mathbf{q}_l(s) = \mathbf{p}_l(s) - \mathbf{f}_l^A(s) - \mathbf{f}_l^B(s) - \cdots - \mathbf{f}_l^Z(s).\end{gathered} \tag{21}$$

If force balance is imposed at each and every node, a matrix equilibrium equation can be formulated as

$$\underline{\mathbf{K}}(s)\mathbf{u}(s) = \mathbf{q}(s), \tag{22}$$

where $\mathbf{u}(s) = \{\mathbf{u}_1^T(s) \cdots \mathbf{u}_N^T(s)\}^T$, $\mathbf{q}(s) = \{\mathbf{q}_l^T(s) \cdots \mathbf{q}_N^T(s)\}^T$, $\underline{\mathbf{K}}(s) = \underline{\mathbf{K}}_{jk}(s)$. Note that $\underline{\mathbf{K}}(s)$, $\mathbf{u}(s)$, and $\mathbf{q}(s)$ are the global stiffness matrix, global nodal displacement and force vectors, respectively.

3.4. IMPOSING BOUNDARY CONDITIONS

Suppose a subsystem is attached at node l has the following prescribed boundary conditions at a point x_i along the subsystem where $x_i < x_l$:

$$\underline{\mathbf{B}}(s)\boldsymbol{\eta}(x_i, s) = \boldsymbol{\kappa}(s). \tag{23}$$

By setting $\boldsymbol{\gamma}(s)$, $\underline{\mathbf{M}}(s)$, and $\underline{\mathbf{N}}(s)$ as

$$\boldsymbol{\gamma}(s) = \begin{Bmatrix}\boldsymbol{\kappa}(s)\\ \boldsymbol{\alpha}(x_l, s)\end{Bmatrix}, \qquad \underline{\mathbf{M}}(s) = \begin{bmatrix}\underline{\mathbf{B}}(s)\\ \underline{\mathbf{0}}\end{bmatrix}, \qquad \underline{\mathbf{N}}(s) = \begin{bmatrix}\underline{\mathbf{0}} & \underline{\mathbf{0}}\\ \underline{\mathbf{I}} & \underline{\mathbf{0}}\end{bmatrix}, \tag{24}$$

the system response for each individual subsystem with the above prescribed boundary conditions is

$$\boldsymbol{\alpha}(x, s) = \int_0^1 \underline{\mathbf{G}}_\alpha(x, \xi, s)\mathbf{f}(\xi, s)\,\mathrm{d}\xi + \underline{\mathbf{H}}_{\alpha 0}(x, s)\boldsymbol{\kappa}(s) + \underline{\mathbf{H}}_{\alpha 1}(x, s)\boldsymbol{\alpha}(x_l, s), \tag{25a}$$

$$\mathbf{P}(x, s) = \underline{\mathbf{E}}(s)\left\{\int_0^1 \underline{\mathbf{G}}_\varepsilon(x, \xi, s)\mathbf{f}(\xi, s)\,\mathrm{d}\xi + \underline{\mathbf{H}}_{\varepsilon 0}(x, s)\boldsymbol{\kappa}(s) + \underline{\mathbf{H}}_{\varepsilon 1}(x, s)\boldsymbol{\alpha}(x_l, s)\right\}. \tag{25b}$$

If $x_i > x_l$, the system response is the same except $\underline{\mathbf{M}}(s)$ and $\underline{\mathbf{N}}(s)$ are now defined by

$$\underline{\mathbf{N}}(s) = \begin{bmatrix}\underline{\mathbf{B}}(s)\\ \underline{\mathbf{0}}\end{bmatrix}, \qquad \underline{\mathbf{M}}(s) = \begin{bmatrix}\underline{\mathbf{0}} & \underline{\mathbf{0}}\\ \underline{\mathbf{I}} & \underline{\mathbf{0}}\end{bmatrix}. \tag{26}$$

4. FLEXIBLE BASE, RIGID EQUIPMENT DESCRIPTION

The system that will be studied is a pinned–pinned aluminum beam of length L, with the isolator mounted along the beam at a distance $x_i = L/3{\cdot}125$ as shown in Figure 2; the mass of the equipment is assumed to be approximately the mass of the base. A detailed discussion of the FBRE system using Yang's method can be found in reference [10].

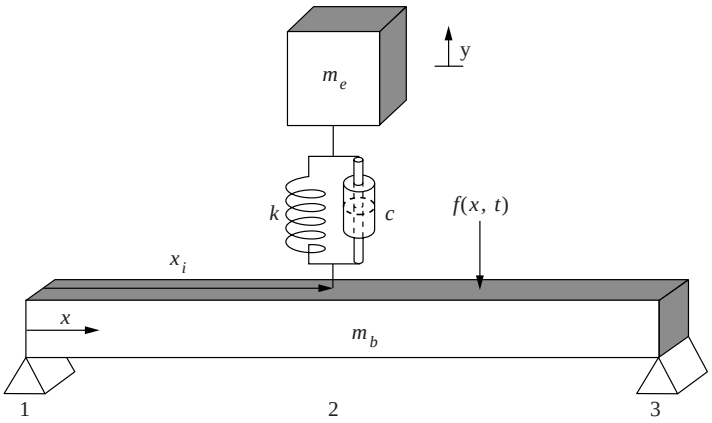

Figure 2. Rigid equipment mounted on flexible base via an isolator.

Assuming that the flexibility in the base will be modeled as a Bernoulli–Euler beam, the governing partial differential equation describing the FBRE system in the domain $\mathscr{D}$: $0 < x < L$ is

$$-EI\frac{\partial^4 w(x,t)}{\partial x^4} + f(x,t) + f_I(x,t) = \rho\frac{\partial^2 w(x,t)}{\partial t^2}. \tag{27}$$

The term $f(x, t)$ is the external force per unit length on the base and the term $f_I(x, t)$ is the force per unit length due to the isolator. It is desired to include damping in the base and the damping will be modeled as proportional damping. A brief discussion on how proportional damping may be included in the above equation is given below. It should be noted that equation (27) was derived by letting the spatial differential operators A, B, and C in equation (1) be ρ, 0, and $EI\,\partial^4/\partial x^4$, respectively.

Assume that the force/unit length term $\mathbf{f}(x, t)$ can be divided into damping forces and non-damping forces. The damping forces are assumed to be proportional to the velocity and are proportional to the linear differential operator B. The damping force/unit length will then be

$$\mathbf{F}_{damp} = -\frac{\partial Bw(x,t)}{\partial t}. \tag{28}$$

It has already been assumed that the damping in the beam will be modeled as proportional damping; so, the linear differential operator B is actually

$$B = \alpha A + \beta C. \tag{29}$$

Substituting this information into equation (27) will lead to the final governing equation for the beam over the domain $\mathscr{D}$: $0 < x < L$:

$$-EI\frac{\partial^4 w(x,t)}{\partial x^4} - \left[\rho\alpha + \beta EI\frac{\partial^4}{\partial x^4}\right]\frac{\partial w(x,t)}{\partial t} + f(x,t) + f_I(x,t) = \rho\frac{\partial^2 w(x,t)}{\partial t^2}. \tag{30}$$

Note that the term $f(x, t)$ is now the external force per unit length that does not include any damping terms. The governing equation of motion for the equipment at the location $x = x_i$ is

$$m_e\ddot{y} = f_I(x, t) = -c\{\dot{y} - \dot{w}(x_i, t)\} - k\{y - w(x_i, t)\}. \tag{31}$$

Equations (30) and (31) are used to develop the overall response for the FBRE system. For example, two subsystems (segments 1–2 and 2–3) and three nodes can be used to describe the system. The significant terms used in Yang's method are

$$\eta(x, s) = \begin{Bmatrix} w(x, s) \\ \dfrac{\partial w(x, s)}{\partial x} \\ \dfrac{\partial^2 w(x, s)}{\partial x^2} \\ \dfrac{\partial^3 w(x, s)}{\partial x^3} \end{Bmatrix}, \qquad \underline{\mathbf{F}}(s) = \begin{bmatrix} 0 & 1 & 0 & 0 \\ 0 & 0 & 1 & 0 \\ 0 & 0 & 0 & 1 \\ \dfrac{-\rho(s+\alpha)s}{EI(1+\beta s)} & 0 & 0 & 0 \end{bmatrix}. \tag{32}$$

5. PASSIVE ISOLATION

For the SDOF model, the mount frequency is designed to have the smallest possible value so that high frequency disturbances will be attenuated as quickly as possible. Therefore, it is desired to discover the effect of base flexibility for various values of isolator stiffness, i.e., mount frequencies. It has also been shown for the SDOF model that isolator damping will decrease the transmissibility at the resonant condition but increase the high frequency transmissibility. Similar results occur when the base is no longer rigid but flexible. The transmissibility (T) for the FBRE system is defined as the displacement (y) of the equipment to the displacement ($w(x, t)$) imposed on the base.

5.1. MOUNT EFFECTIVENESS

For the following analysis, it is assumed that the base and isolator have no damping and the mount frequency of the isolator is defined as $w_o = \sqrt{k/m_e}$, where k is the isolator stiffness and m_e is the equipment mass. Table 1 is a list of the flexible base, rigid equipment (FBRE) frequencies for various isolator mount frequencies. If the mount frequency is much lower than the first mode of the base (low-frequency mount design), the FBRE

TABLE 1

FBRE frequencies for varying mount frequencies

		Mount frequency (Hz)		
Mode	No mount	7·1176	22·5079	71·1762
1	56·5800	7·0177	19·6002	31·7227
2	226·3200	57·3269	64·3001	113·2115
3	509·2202	226·5334	228·4943	251·5864
4	905·2822	509·2208	509·2386	509·4171
5	1414·5090	905·3208	905·6690	909·2033
6	2036·9077	1414·5467	1414·8861	1418·3245
7	2772·2491	2036·9095	2036·9256	2037·0881

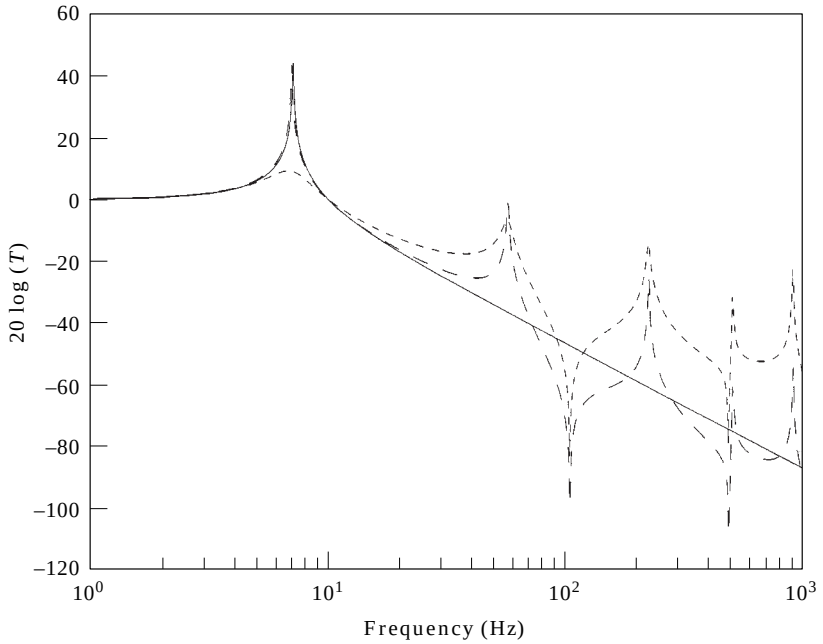

Figure 3. Influence of isolator damping of FBRE system with $f_o = 7{\cdot}1176$ Hz (−, rigid base and equipment; —, passive damping $\zeta = 0$; --, passive damping $\zeta = 0{\cdot}2$).

system will have natural frequencies corresponding to the concatenation of the mount frequency and the beam frequencies. The mount frequency becomes the first FBRE mode, the first base mode is the second FBRE mode, the second base mode is the third FBRE mode, etc. Note that the first mode of the FBRE system will be slightly smaller than the mount frequency for a low-frequency mount design. However as the mount frequency is designed closer to the first mode of the base, the modes of the FBRE system start to shift. For a mount frequency designed at $f_o = 22{\cdot}51$ Hz, the FBRE system will have a first mode 13% less than the mount frequency; the rest of the FBRE modes will be slightly higher than the base frequencies given in Table 1 under the heading "No Mount".

Somewhat different results are obtained when the mount frequency is designed between the base modes; this system will be referred to as the mid-frequency mount design. For example, consider the case when the mount frequency is designed at $f_o = 71{\cdot}18$ Hz; the value of the mount frequency lies between the first two modes of the base. The new frequency that is added to the FBRE system due to the isolator mount is no longer near the mount frequency. In fact, the new mode of the FBRE system due to the isolator mount is 113·21 Hz; this mode has shifted by 59%. There has also been a dramatic shift of the base frequencies that are close to the mount frequency. The first mode of the FBRE system has shifted from the base frequency of 56·58 to 31·72 Hz (44%) and the third mode of the FBRE system has shifted from 226·32 to 251·59 Hz (11%). The significance of this interaction will be demonstrated when the isolator includes damping.

5.2. INFLUENCE OF ISOLATOR DAMPING

It was shown in the previous section that when the mount frequency is designed lower than any of the base modes, the natural frequencies of the FBRE system is a concatenation of the mount frequency and the base frequencies. Since the mount frequency has very little

or no effect on the higher-order base modes, the inclusion of isolator damping will have an effect on only the first mode. Remember that the first mode of the FBRE system is due to the addition of the isolator and equipment to the base. Figure 3 shows the influence of isolator damping for a low-frequency mount design at $f_o = 7{\cdot}12$ Hz. As seen from this figure, the FBRE model with no damping is similar to an undamped SDOF model except for the infinite number of modes present at the higher frequencies. The FBRE transmissibility decreases at a rate of 40 dB/decade after reaching the first mode which is similar to the SDOF system. Also, as the damping is increased in the FBRE system, the transmissibility of the first FBRE mode is attenuated, but the transmissibility at the other frequencies is increased.

A different situation occurs when the mount frequency is designed between two of the base modes. It was shown in the previous section that this type of design will have a significant impact on the system's frequencies. Figure 4 shows the influence of this interaction when isolator damping is included for a system having a mid-frequency mount designed at $f_o = 71{\cdot}18$ Hz. This figure shows that attenuation in the first three modes have occurred. The most significant attenuation occurs in the second mode since this mode is due to the addition of the isolator and equipment to the base. The first and third modes are attenuated as well, but not as significantly as the second mode. One significant drawback in this design is that the transmissibility does not decrease at a rate of 40 dB/decade until the second mode. Therefore, the transmissibility will not be significantly attenuated in the high frequency ranges compared to a low-frequency mount design, as shown in Figure 3. A low-frequency mount design will also have more attenuation in the first mode than a mid-frequency mount design. This is expected since the first mode for the low-frequency mount system corresponds to the addition of the isolator.

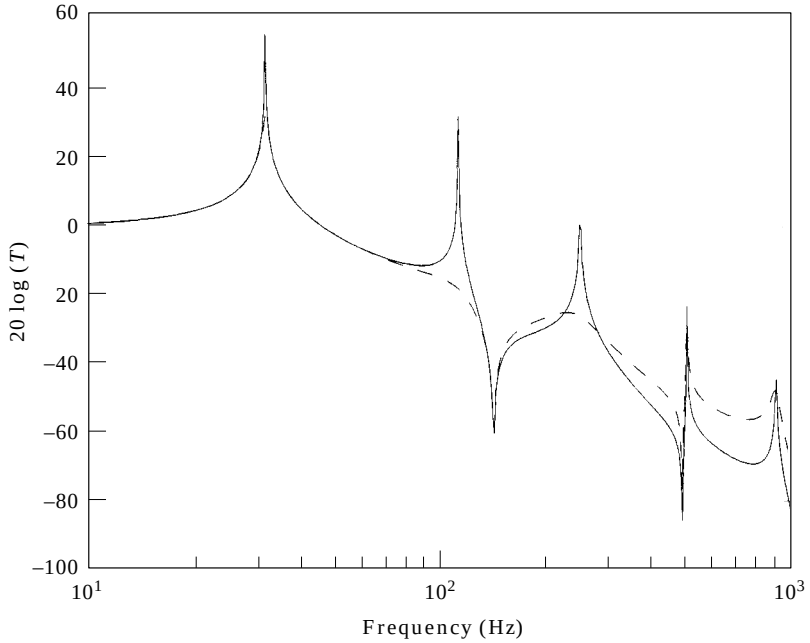

Figure 4. Influence of isolator damping of FBRE system with $f_o = 71{\cdot}1762$ Hz (−, passive isolation $\zeta = 0$; —, passive isolation $\zeta = 0{\cdot}2$).

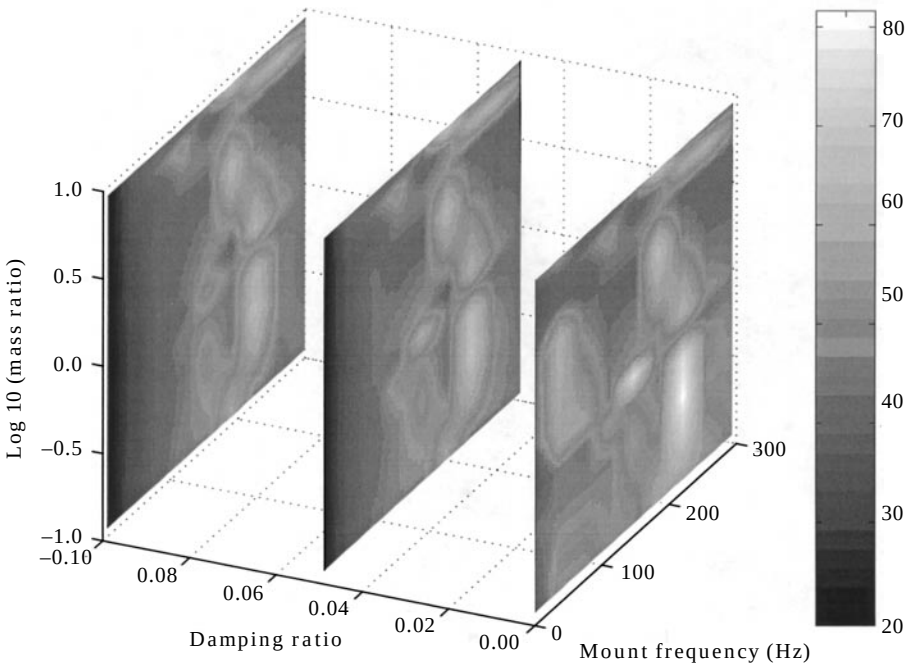

Figure 5. Influence of isolator damping and mount frequency.

5.3. VARYING MOUNT FREQUENCIES AND ISOLATOR DAMPING

The previous sections discuss that a mid-frequency isolator mount should be used since it can attenuate multiple modes when damping is presented in the isolator. However, the drawback with this design is that the transmissibility will not decrease at a rate of 40 dB/decade until after the mount frequency is reached. Also, as the amount of passive damping in the isolator is increased, the transmissibility of the system is increased in the higher frequency ranges. Therefore, a trade-off between mount frequency designs should be made when damping is present in the isolator.

This section will look at various isolator designs where three independent variables are varied simultaneously: the equipment mass relative to the base mass, the isolator damping, and the isolator mount frequency. This can be a very difficult problem to analyze for a wide range of parameters and an approach by Sciulli [10] eliminates the complexity for this type of analysis. This approach is used to find isolator design trends rather than finding exact solutions to the problem. Briefly stated, the transmissibility of the system is determined for the varying parameters and the root-mean-square (r.m.s.) of the transmissibility is determined. The r.m.s. values of the transmissibility are then converted to decibels and color coded depending on their value; low r.m.s. values are represented by a black color and high r.m.s. values are represented by a white color. Values in between are shaded according to the high and low r.m.s. values. The r.m.s. values are then plotted in three dimensions with a color bar indicating values of the r.m.s. transmissibility for each independent variable.

The FBRE system that will be studied will have the isolator mount frequency ranging from 7 to 300 Hz, the isolator damping ratio ranging from 0·001 to 0·1, and the equipment mass ranging from ten times smaller to ten times larger than the base mass. For this system, structural damping in the base was neglected and the results are shown in Figure 5. As expected, low-frequency mounts, which are defined by mount frequencies designed much

lower than the lowest base mode, tend to perform best in an overall sense. The higher mount frequencies, that is mount frequencies greater than the first base mode, tend to perform poorly compared to low-frequency isolator mounts at equal isolator damping. However, mid-frequency mounts with significant damping tend to perform equally well compared to a low-frequency mount with minimal amount of damping. The mid-frequency mounts do not include areas where the transmissibility is significantly high.

6. ACTIVE ISOLATION

Active control for the flexible base, rigid equipment (FBRE) system is divided into two major parts. The first part is to determine the best placement of the sensor. That is, should the sensor be placed on the equipment that is to be isolated or on the flexible base. The second part will implement three different control strategies on the FBRE system. The control laws that will be used are proportional-plus-integral-plus-derivative ($\mathscr{PID}$) controller [11, 12], a linear quadratic Gaussian (LQG) controller [13–15], and positive position feedback (PPF) controller [16]. The control laws will be used to analyze the transmissibility when the mount frequency is designed at $f_o = 71{\cdot}18$ Hz and base damping will be neglected. The transmissibility for the FBRE system is defined as the displacement of the equipment due to the disturbance at the base.

6.1. SENSOR LOCATION

For a SDOF model, velocity feedback does not increase the high frequency transmissibility, but does add damping at the resonant condition. Similar results can be obtained for the FBRE system depending on the sensor location. For the FBRE system, the active controller will implement velocity feedback when no form of passive damping is present in the isolator. The controller will try to add 20% damping to the first mode,

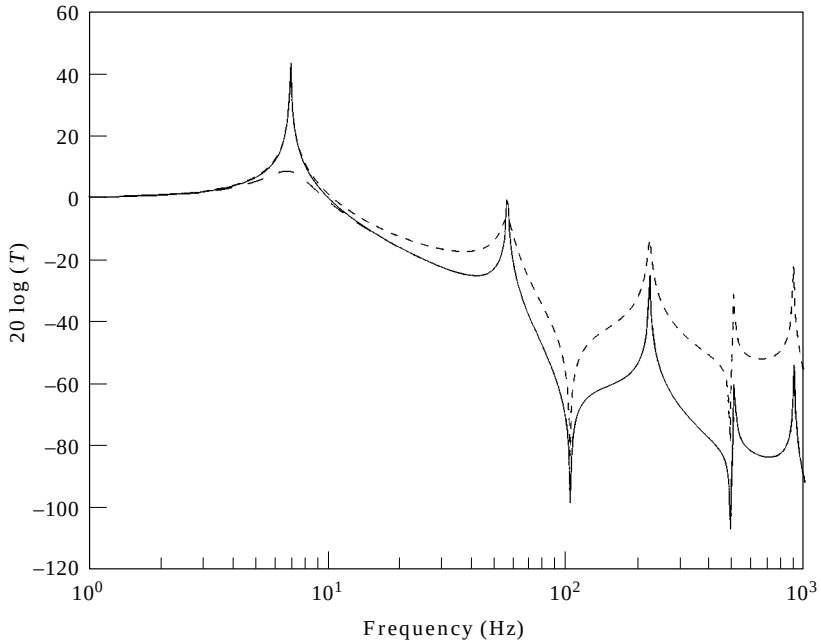

Figure 6. Comparison of feedback control from equipment and base (−, passive, no damping; —, feedback from equipment; --, feedback from base).

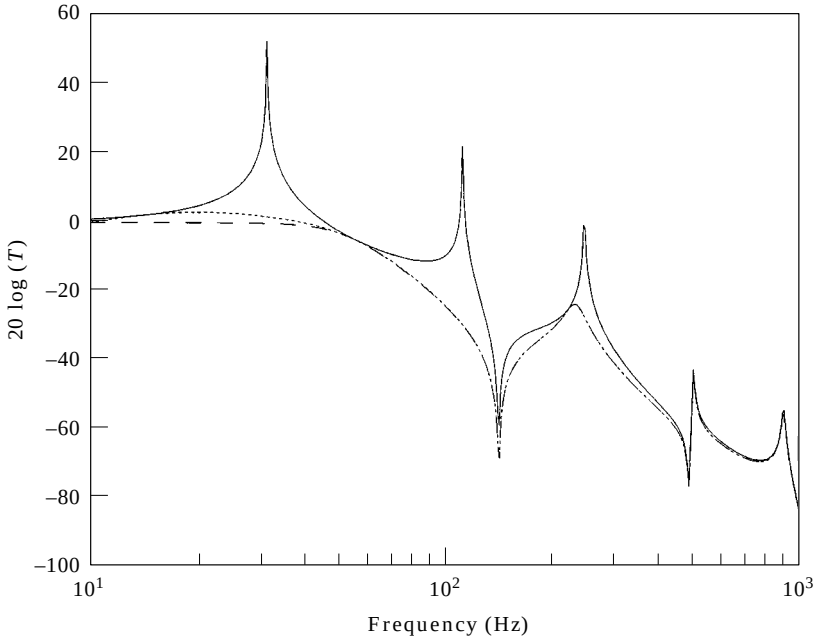

Figure 7. Transmissibility for FBRE system using PID control (−, no control; —, PID control; --, PD control).

so a comparison can be made to the results obtained from the previous sections on passive isolation. A mount design at $f_o = 7{\cdot}12$ Hz is used since a design at $f_o = 71{\cdot}18$ Hz will give similar results.

When base feedback is used, the first mode of the FBRE system will be lightly damped and the transmissibility at higher frequencies will be increased, as shown in Figure 6. This is similar to the situation when passive damping is present in the isolator with one significant difference being the amount of damping in the first mode. A small amount of damping is present for the active system compared to the passive system; the active system has a transmissibility of 40 dB (Figure 6) at the first mode while the passive system has a transmissibility of about 8 dB (Figure 3). Therefore, for base feedback the passive system dramatically outperforms the active system.

Different results are obtained when the sensor is located on the equipment. The first mode is significantly attenuated compared to base feedback. Actually, the amount of damping at the first mode is comparable to the system with passive damping in the isolator (Figure 3). Also, the transmissibility at higher frequencies for the active isolator tracks an undamped isolation system. The results in using equipment feedback are similar to a SDOF model with the main difference being the inclusion of an infinite number of modes in the FBRE system. Therefore, all control architectures used in the FBRE system should use equipment feedback if the goal is to isolate the equipment from base disturbances.

The choice of sensor placement is consistent with an observability index approach developed by Hughes and Skelton [17]. They developed a procedure to determine observability indices for each system mode; the indices can then be ranked according to their magnitudes. This ranking can then be used to determine the most beneficial sensor location [18]. For instance, the observability indices of the first FBRE mode for base and equipment feedback are $\mathcal{O}_1^b = 0{\cdot}1247$ and $\mathcal{O}_1^e = 4{\cdot}4712$, respectively. Since the observability index for equipment feedback is greater than the observability index for base feedback, the best sensor location is on the equipment.

6.2. $\mathscr{PID}$ CONTROL

The first control architecture that will be implemented is a proportional-plus-integral-plus-derivative ($\mathscr{PID}$) controller. The form of the controller in the Laplace domain is

$$F(s) = (K_P + K_D s + K_I/s)Y(s), \tag{33}$$

where $Y(s)$ is the displacement of the equipment, and K_P, K_D, and K_i are the proportional, derivative, and integral gains, respectively. The gain for the proportional control was chosen such that it would not affect the frequencies of the system. The derivative gain was chosen to give a fast rise time with as little overshoot as possible, and the integral gain was chosen to give good system error and settling time. The frequency response function is shown in Figure 7. With a simple $\mathscr{PID}$ controller and having the mount frequency designed between two base modes, the transmissibility will be simultaneously attenuated at three different modes where the second mode exhibits the most damping. This is attributable to the fact that this mode corresponds to the addition of the isolator and equipment to the base. Significant attenuation of the first and third modes is also accomplished.

6.3. LINEAR QUADRATIC GAUSSIAN CONTROL

Another controller that was used was the linear quadratic Gaussian (LQG) regulator. This controller minimizes a quadratic cost function with respect to the states of the system and the control input. For this controller, it is assumed that all the states are not known so a Kalman–Bucy filter is used as an estimator. It is also assumed that the form of the disturbance is known, and a shaping filter is used to model the disturbance. For comparison to $\mathscr{PID}$ control, it is assumed that the disturbance occurs at the second mode, and the results obtained using LQG control are shown in Figure 8. These results are similar to the $\mathscr{PID}$ control shown in Figure 7 where the first three modes of the FBRE system

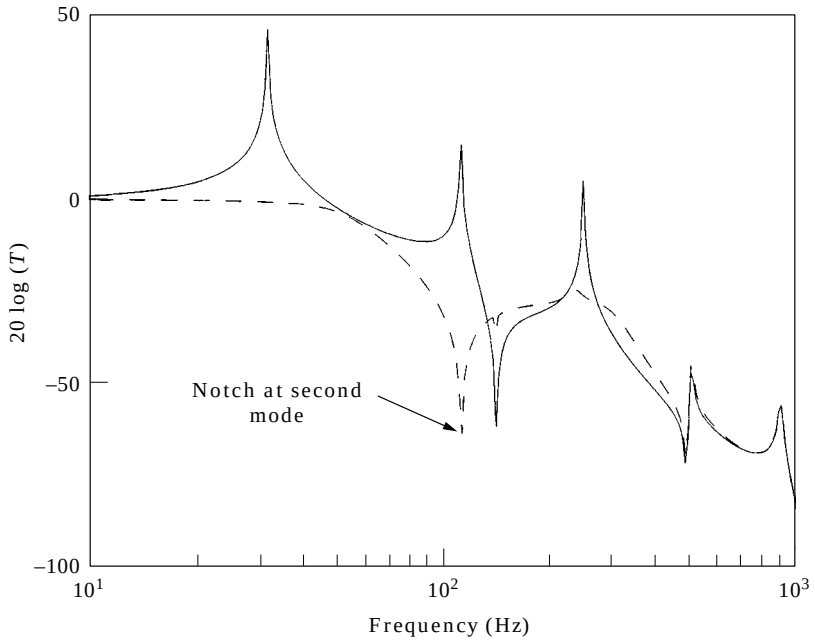

Figure 8. Transmissibility for FBRE system using LQG control (−, passive isolation; —, LQG control).

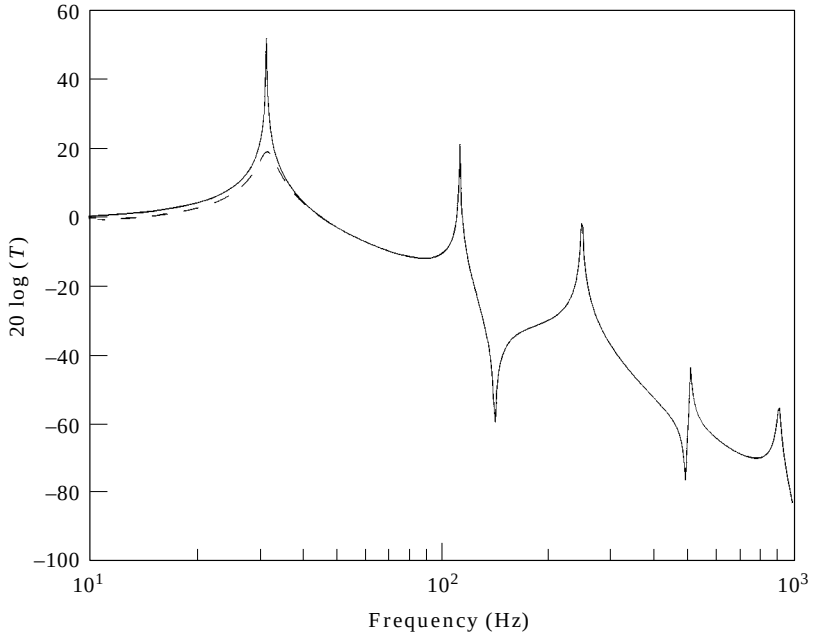

Figure 9. Transmissibility for FBRE system using PPF control (−, no control; —, PPF control).

are attenuated. The major difference between the LQG control and $\mathscr{PID}$ control is the notch that occurs at the second mode using a LQG regulator.

6.4. POSITIVE POSITION FEEDBACK CONTROL

$\mathscr{PID}$ and LQG control have been shown to be quite effective, especially when the modes are coupled. However, there may be situations where it is desired to attenuate only one mode. A control methodology that can accomplish this is a positive position feedback (PPF) controller. The PPF controller is basically a second-order filter in the form

$$\ddot{\eta} + 2\zeta_f \omega_f \dot{\eta} + \omega_f^2 = \omega_f^2 \xi, \tag{34}$$

where ξ is the structural modal coordinate, η is the filter coordinate, ω_f is the filter frequency, and ζ_f is the filter damping ratio. The filter coordinate is applied to the structure by the value $g\omega^2\omega_f^2$, where g is the gain and ω is a mode of the structure. By proper choice of ζ_f and ω_f, the PPF controller can be used to attenuate any specific mode of the structure.

The PPF filter was designed to attenuate the transmissibility at the first mode. The gain, the filter frequency and damping ratio for the PPF compensator were chosen to give adequate attenuation at the first mode. The results with the PPF filter are shown in Figure 9 and about 30 dB of attenuation of the mode was achieved. Even though the modes are highly interactive for this mid-frequency mount design, the PPF filter does not affect any of the other modes. This can be attributed to the fact that the attenuation is accomplished through position feedback and not velocity feedback.

7. CONCLUSIONS

A method developed by Yang was used to find an analytical solution to a system that has some flexible members. This method is then used to examine various design possibilities

for vibration isolation when flexibility is important. Using this method, it was determined that the design of the mount frequency will have a significant impact in the isolation design. If the mount frequency is designed between two modes of the flexible base, a coupling condition will exist between the affected modes. When damping is included in the isolator, this coupling will simultaneously damp three modes instead of the usual one mode. With the use of active controllers such as $\mathscr{PID}$ or LQG, the coupled modes can be significantly attenuated compared to a passive isolation approach. It has also been shown that a PPF controller will not attenuate three modes. This is due to the fact that the structural position is used as feedback to the actuator. Therefore, the interaction of modes for a mid-frequency mount design is due to velocity feedback.

It has also been shown that when an active isolator is implemented, it is desired to place the feedback sensor on the equipment. If the sensor is placed on the base, the high frequency transmissibility is increased similar to a system implementing passive isolation; feedback from the equipment does not have this result. The amount of attenuation in the first mode is significantly greater when feedback occurs from the equipment than the base.

ACKNOWLEDGMENTS

The first author would like to acknowledge the USAF Palace Knight Program for their support. The second author gratefully acknowledges the support of the AFOSR.

REFERENCES

1. C. M. Harris 1988 *Shock & Vibration Handbook*. New York: McGraw-Hill; third edition.
2. F. C. Nelson 1994 *Shock and Vibration* **5**, 485–493. Vibration isolation: a review, I. Sinusoidal and random excitations.
3. D. C. Karnopp 1995 *Journal of Vibration and Acoustics* **117**, 177–185. Active and semi-active vibration isolation.
4. A. H. von Flotow 1988 *Proceedings of the 27th Conference on Decision and Control* **3**, 2029–2032. An expository overview of active control of machinery mounts.
5. G. H. Blackwood and A. H. von Flotow 1993 *Technical Report SERC #* 13-93. M.I.T. Space Engineering Research Center. Active vibration isolation for controlled flexible structures.
6. J. C. Snowdon 1973 *Acustica* **28**, 307–317. Isolation and absorption of machinery vibration.
7. B. Yang 1994 *Journal of Applied Mechanics* **61**, 84–92. Distributed transfer function analysis of complex distributed parameter systems.
8. L. Meirovitch 1986 *Elements of Vibration Analysis*. New York: McGraw-Hill; second edition.
9. A. O. Sykes 1987 *National Aeronautics and Space Administration*. 58*th Shock and Vibration Symposium*, 411–439. Passive vibration-cancellation isolation mount.
10. D. Sciulli 1997 *Ph.D. Dissertation*, *Virginia Polytechnic Institute and State University*. Dynamics and control for vibration isolation design.
11. G. F. Franklin, J. D. Powell and A. Emami-Naeini 1991 *Feedback Control of Dynamic Systems*. New York: Addison Wesley; second edition.
12. V. J. Bucek 1989 *Control Systems*: *Continuous and Discrete*. Englewood Cliffs, NJ: Prentice-Hall; first edition.
13. L. A. Sievers and A. H. von Flotow 1988 *Procedings of the 27th Conference on Decision and Control* **2**, 1032–1037. Linear control design for active vibration isolation of narrow band disturbances.
14. T. T. Hyde and E. F. Crawley 1995 *Proceedings of the American Control Conference* **5**, 3835–3839. H_2 synthesis for active vibration isolation.
15. B. D. O. Anderson and J. B. Moore 1990 *Optimal Control*: *Linear Quadratic Methods*. Englewood Cliffs, NJ: Prentice-Hall; first edition.
16. J. L. Fanson and T. K. Caughey 1987 *AIAA Dynamics Specialist Conference*, 588–317. Positive position feedback control for large space structures.

17. P. C. HUGHES and R. E. SKELTON 1980 *Journal of Applied Mechanics* **47**, 415–420. Controllability and observability of linear matrix-second-order systems.
18. P. C. HUGHES and R. E. SKELTON 1980 *Journal of Guidance and Control* **3**, 452–459. Controllability and observability for flexible spacecraft.

APPENDIX: NOMENCLATURE

EI	Young's modulus × area moment of inertia
$\underline{\mathbf{I}}$	identity matrix
$\underline{\mathbf{M}}(s)$	boundary condition matrix at left end of a particular subsystem
$\underline{\mathbf{N}}(s)$	boundary condition matrix at right end of a particular subsystem
$\mathbf{P}(x, s)$	local internal force vector
$\mathbf{Q}_k^\delta$	global force vector of subsystem δ at node k
$\underline{\mathbf{R}}^\delta$	transformation matrix of local forces to global forces for subsystem δ
$\underline{\mathbf{S}}^\delta$	transformation matrix of local displacements to global displacements for subsystem δ
$\underline{\mathbf{T}}^\delta$	transformation matrix of local displacements to global displacements for subsystem δ
$\underline{\mathbf{0}}$	zero matrix
c	isolator coefficient of damping
$\mathbf{f}(x, \_)$	external force/unit length on subsystem in the time or Laplace domain
$\mathbf{f}_I(x, \_)$	point force/unit length due to the isolator
k	isolator stiffness
m_e	equipment mass
$w(x, \_)$	vertical deflection of base or vertical deflection of distributed system in the time or Laplace domain
$y, \dot{y}, \ddot{y}$	displacement, velocity and acceleration of equipment
α	proportional damping term for base
$\boldsymbol{\alpha}(x, s)$	local displacement vector for a particular subsystem
β	proportional damping term for base
$\boldsymbol{\varepsilon}(x, s)$	local strain vector for a particular subsystem
$\boldsymbol{\gamma}(\_)$	external disturbances at the boundaries in the time or Laplace domain
ρ	mass per unit length
$\boldsymbol{\eta}(x, s)$	solution vector for distributed system
$\boldsymbol{\zeta}$	damping ratio of isolator defined as $c/(2\sqrt{km_e})$